

RESEARCH

Open Access



Variable pilot assisted channel estimation in MIMO-OFDM system with STBC and different modulation modes

Qun Wu, Xiao Zhou, Chengyou Wang and Hai Cao 

*Correspondence:
caohai@sdu.edu.cn

School of Mechanical,
Electrical and Information
Engineering, Shandong
University, Weihai 264209,
China

Abstract

High speed and low latency have become the development trend of mobile communication network. Orthogonal frequency division multiplexing (OFDM) technology has become the key technology of mobile communication network due to its efficient transmission method. Space time block coding (STBC) introduces time and space correlation in the signals sent by different antennas, so that diversity gains and coding gains are obtained for the multiple input multiple output-OFDM (MIMO-OFDM) receiver without sacrificing bandwidth. STBC is a signal coding technology that combines higher transmission rates and it is a combination of space and time transmission signals. STBC uses the spatial diversity of multiple transmitters and multiple receivers in space to improve the capacity and information rate of the OFDM system. It proceeds parallel multiplex transmission in the transmission channel, which effectively improves spectrum utilization. For obtaining diversity gains and spectrum efficiency, this paper introduces a variable pilot assisted channel estimation method with different modulation modes. In this paper, the new type pilot sequences with different modulation orders are proposed for improving spectrum efficiency. The proposed variable pilot assisted channel estimation method in MIMO-OFDM systems is adopted with different low and high order modulations. Simulation results show that the proposed variable pilot assisted channel estimation method has 1–2 dB signal-to-noise ratio (SNR) gains for bit error rate (BER) performance of MIMO-OFDM systems.

Keywords: Orthogonal frequency division multiplexing (OFDM), Space time block coding (STBC), Additive white Gaussian noise (AWGN), Multiple input multiple output (MIMO), Bit error rate (BER)

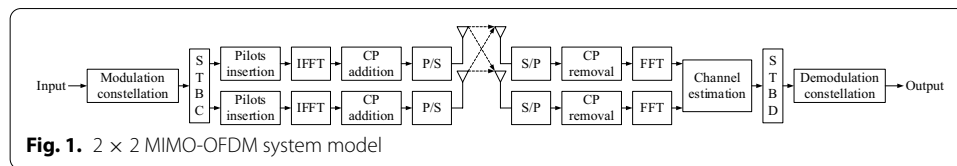
1 Introduction

Orthogonal frequency division multiplexing (OFDM) system is characterized by its robustness to the multipath induced inter-symbol interference (ISI) [1, 2]. Foschini et al. [3, 4] proved that antenna diversity can be exploited to significantly enhance channel capacity by using multiple antennas at both transmitter and receiver. Recently, space time block coding (STBC) and space time block decoding (STBD) have been proposed as an efficient way to achieve this capacity improvement for the

multiple input multiple output-OFDM (MIMO-OFDM) system, which is recognized as the promising technology for 5G and 6G mobile communications.

In MIMO-OFDM systems, like STBC-based transmit diversity system, channel state information (CSI) [5] is required for coherent detection and decoding. CSI can be obtained in two categories. The one does not require pilots, and the other is based on pilots which are known beforehand at the receiver. In STBC MIMO-OFDM systems, symbols are transmitted from different antennas simultaneously, and the received signal is the superposition of these signals. The designed pilot sequence is orthogonal among transmitting antennas [6]. Optimal pilot sequences were proposed in [7, 8] for MIMO-OFDM systems. Chern et al. [9] proposed a new pseudo random cyclic postfix-OFDM system, but the disadvantage is that the cyclic postfix sacrifices the frequency bandwidth. Del Peral-Rosado et al. [10] proposed an optimal placement of the pilot subcarriers about the mean square error (MSE) of the least square (LS) channel estimation for single input single output-OFDM systems. Younas et al. [11] proposed the MIMO-OFDM system based on adaptive LS channel estimation method with pilot aided sequences in the correlated time varying channels. It simplifies the LS channel estimation by utilizing the proposed pilot construction, which avoids matrix inversion. Linear minimum mean square error and singular value decomposition channel estimation methods are widely utilized in multi-user MIMO-OFDM systems [12, 13], but they inevitably bring many matrix calculations in frequency domain.

For virtual multiple input single output-OFDM systems, Wang et al. [14] proposed an efficient resource allocation method to provide high transmission throughput. The base station allocates subcarriers to transmit node with the highest magnitude of channel frequency response (CFR) on the subcarriers. In time varying channels, Youssefi et al. [15] proposed a new approach to achieve optimal training sequences (OTS) in terms of minimizing the MSE for spectrally efficient MIMO-OFDM systems. The OTS are equal powered and spaced, and orthogonal positioned. However, in practical OFDM based systems with low pass filter, to avoid the transmitted signals being distorted, the subcarriers that fall in the roll-off region of the filter are usually not used, which are often referred to as virtual subcarriers [16, 17]. The existence of virtual subcarriers breaks the equal spaced property of conventional pilot sequences and the system performance can be increased. Kenarsari-Anhari et al. [18] formulated the power allocation as linear programming problem in coded OFDM systems. Wang et al. [19] proposed a low complexity power allocation method in the cooperative OFDM networks which greatly improves the system throughput. The equivalent channel power gain is calculated and the power among each subcarrier is allocated through Lagrange optimization method. In MIMO-OFDM systems, the frequency resources are very valuable and sparse. To improve the reliability of communication and spectrum efficiency, the paper proposes a variable pilot sequence assisted channel estimation method in MIMO-OFDM system, which suppresses the ISI and inter-carrier interference (ICI) in time and spatial distribution effectively. Our main contributions are as follows: (1) We propose a method that can change the pilot insertion interval according to the modulation order of the signal, which can flexibly utilize spectrum resources and flexibly select the pilot amplitude. (2) We combine STBC and variable pilot method, which can be applied to different modulation schemes, such as



binary phase shift keying (BPSK), quadrature phase shift keying (QPSK), 8-phase shift keying (8PSK), 16-quadrature amplitude modulation (16QAM), and 64-quadrature amplitude modulation (64QAM). (3) Simulation results are provided to demonstrate the effectiveness and superiorities of the proposed method and it show that the proposed variable pilot assisted channel estimation method has 1–2 dB signal-to-noise ratio (SNR) gains for bit error rate (BER) performance of MIMO-OFDM systems.

The remainder of this paper is organized as follows. The MIMO-OFDM system model is presented in Section 2. Section 3 introduces variable pilot assisted channel estimation. Section 4 illustrates simulation results and comparison analysis. Section 5 concludes the paper.

2 MIMO-OFDM system model

Figure 1 illustrates the 2×2 MIMO-OFDM system model, at the transmitter, the input bits are grouped and mapped according to a pre-specified constellation modulation scheme, which likes BPSK, QPSK, 8PSK, 16QAM, and 64QAM [20] that the modulation order ε is 1, 2, 3, 4, and 6, respectively. The higher order modulation mode is, the more bits an OFDM symbol carries and the more information the MIMO-OFDM system transmits. That is, higher order modulation improves the transmission efficiency of MIMO-OFDM. In this paper, the modulation order of 1, 2, 3, 4, 6 is considered in the MIMO-OFDM system. However, high order modulation causes a problem that phase interference occurs during symbols demodulation among different constellation points, resulting in demodulation errors among some signals. However, the combination of STBC and OFDM technology overcomes the disadvantage effectively.

2.1 System model

Figure 2 illustrates pilot allocation in time, frequency, and space in STBC MIMO-OFDM system. Due to the superimposed noise on the signals and pilots in the time, frequency, space domains, and the mutual interference among the transmitting and receiving antenna pairs, there induces inevitable mistakes among the transmitting and receiving signals. These mistakes are reduced by different modulation methods and pilot intervals. After constellation modulation, the modulated symbols are sent to space-time encoder. After STBC in the transmitter, the comb type pilots are inserted with fixed intervals of subcarriers. As shown in Fig. 1, the inverse fast Fourier transform (IFFT) converts \mathcal{S}_1 and \mathcal{S}_2 from frequency domain to time domain, denoted as s_1 and s_2 , respectively. The time domain signals can be expressed as:

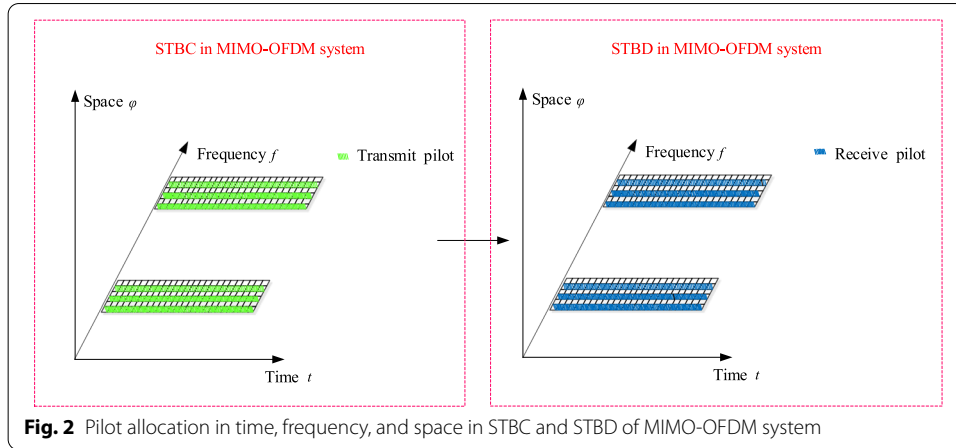


Fig. 2 Pilot allocation in time, frequency, and space in STBC and STBD of MIMO-OFDM system

$$s_{\alpha}(n) = \frac{1}{\sqrt{N}} \sum_{k=0}^{N-1} S_{\alpha}(k) e^{j\frac{2\pi kn}{N}}, \quad 0 \leq k \leq N - 1, \tag{1}$$

where $\alpha = 1, 2$ is the index of transmitting antennas, N is length of IFFT, k is the index of subcarriers.

At receiver, the received frequency domain signals can be expressed as:

$$Y_{\beta}(k) = \sum_{\alpha=1}^2 H_{\alpha,\beta}(k) S_{\alpha}(k) + W(k), \quad 0 \leq k \leq N - 1, \tag{2}$$

where $\beta = 1, 2$ is the index of receiving antennas, $W(k)$ is the additive white Gaussian noise (AWGN) of the wireless channels. After removing the cyclic prefix (CP), the time domain received OFDM signals are transformed into frequency domain by fast Fourier transform (FFT), which can be expressed as:

$$Y_{\beta}(k) = \frac{1}{\sqrt{N}} \sum_{n=0}^{N-1} y_{\beta}(n) e^{-j\frac{2\pi kn}{N}}, \quad 0 \leq n \leq N - 1. \tag{3}$$

In the receiver of MIMO-OFDM system, the frequency domain symbols are decoded in STBD decoder. The signals at multiple receiving antennas are decoded using CSI provided by the channel equalizer. Therefore, channel equalizer is a critical module of MIMO-OFDM systems. At last, the binary information bits are obtained after the BPSK, QPSK, 8PSK, 16QAM, and 64QAM constellation demodulation.

2.2 STBC and STBD

According to Alamouti criterion, the space-time coded signals are allocated to two antennas. After STBC [2], the transmitted OFDM codeword is expressed as:

$$S = \begin{bmatrix} S(i) & -S(i+1)^* \\ S(i+1) & S(i)^* \end{bmatrix}, \tag{4}$$

where i denotes the i th OFDM symbol; $(\cdot)^*$ denotes the conjugation operation. According to Eq. (4), the transmitting OFDM symbol on the first transmitting antenna is expressed as:

$$\mathbf{S}_1 = [\mathbf{S}(i) \ -\mathbf{S}(i+1)^*]. \tag{5}$$

Correspondingly, the transmitting OFDM symbol on the second transmitting antenna is expressed as:

$$\mathbf{S}_2 = [\mathbf{S}(i+1) \ \mathbf{S}(i)^*]. \tag{6}$$

Diversity gains can be obtained by using STBC technology at the transmitter. STBC is a key technology to improve the reliability of MIMO-OFDM systems.

According to the estimated CFR, the OFDM symbols after STBD in the receiver can be expressed as:

$$\begin{bmatrix} \hat{\mathbf{S}}(i) \\ \hat{\mathbf{S}}(i+1) \end{bmatrix} = \begin{bmatrix} \frac{Y_1(i)\hat{\mathbf{H}}_{1,1}^*(i) + Y_1^*(i+1)\hat{\mathbf{H}}_{2,1}(i) + Y_2(i)\hat{\mathbf{H}}_{1,2}^*(i) + Y_2^*(i+1)\hat{\mathbf{H}}_{2,2}(i)}{\hat{\mathbf{H}}_{1,1}(i)\hat{\mathbf{H}}_{1,1}^*(i) + \hat{\mathbf{H}}_{2,1}(i)\hat{\mathbf{H}}_{2,1}^*(i) + \hat{\mathbf{H}}_{1,2}(i)\hat{\mathbf{H}}_{1,2}^*(i) + \hat{\mathbf{H}}_{2,2}(i)\hat{\mathbf{H}}_{2,2}^*(i)} \\ \frac{Y_1(i)\hat{\mathbf{H}}_{2,1}^*(i) - Y_1^*(i+1)\hat{\mathbf{H}}_{1,1}(i) + Y_2(i)\hat{\mathbf{H}}_{2,2}^*(i) - Y_2^*(i+1)\hat{\mathbf{H}}_{1,2}(i)}{\hat{\mathbf{H}}_{1,1}(i)\hat{\mathbf{H}}_{1,1}^*(i) + \hat{\mathbf{H}}_{2,1}(i)\hat{\mathbf{H}}_{2,1}^*(i) + \hat{\mathbf{H}}_{1,2}(i)\hat{\mathbf{H}}_{1,2}^*(i) + \hat{\mathbf{H}}_{2,2}(i)\hat{\mathbf{H}}_{2,2}^*(i)} \end{bmatrix}. \tag{7}$$

Simplifying Eq. (7), we can obtain:

$$\begin{bmatrix} \hat{\mathbf{S}}(i) \\ \hat{\mathbf{S}}(i+1) \end{bmatrix} = \begin{bmatrix} \frac{\hat{Y}_1(i)\hat{\mathbf{H}}_{1,1}^*(i) + \hat{Y}_1^*(i+1)\hat{\mathbf{H}}_{2,1}(i) + \hat{Y}_2(i)\hat{\mathbf{H}}_{1,2}^*(i) + \hat{Y}_2^*(i+1)\hat{\mathbf{H}}_{2,2}(i)}{|\hat{\mathbf{H}}_{1,1}(i)|^2 + |\hat{\mathbf{H}}_{2,1}(i)|^2 + |\hat{\mathbf{H}}_{1,2}(i)|^2 + |\hat{\mathbf{H}}_{2,2}(i)|^2} \\ \frac{\hat{Y}_1(i)\hat{\mathbf{H}}_{2,1}^*(i) - \hat{Y}_1^*(i+1)\hat{\mathbf{H}}_{1,1}(i) + \hat{Y}_2(i)\hat{\mathbf{H}}_{2,2}^*(i) - \hat{Y}_2^*(i+1)\hat{\mathbf{H}}_{1,2}(i)}{|\hat{\mathbf{H}}_{1,1}(i)|^2 + |\hat{\mathbf{H}}_{2,1}(i)|^2 + |\hat{\mathbf{H}}_{1,2}(i)|^2 + |\hat{\mathbf{H}}_{2,2}(i)|^2} \end{bmatrix}, \tag{8}$$

where $\hat{\mathbf{S}}(i)$ is the i th symbol after STBD; $Y_\beta(i)$ ($\beta = 1, 2$) is the i th symbol received by the β th receiving antenna; $\hat{\mathbf{H}}_{\alpha,\beta}$ ($\alpha = 1, 2, \beta = 1, 2$) is the estimated CFR between α th transmitting antenna and β th receiving antenna.

3 Variable pilot assisted channel estimation

3.1 Various comb-type pilot sequences

The comb pilot interval can be selected according to the frequency selectivity or time selectivity of the fading environment. When the total subcarrier number $N = 2048$, there are six options for pilot interval n , which are 2, 4, 8, 20, 50, and 100, respectively. Figure 3 shows the optional comb type pilot, where (a–d) represent comb type pilot $\mathbf{x}_1, \mathbf{x}_2, \mathbf{x}_3$, and \mathbf{x}_4 , respectively. Assuming the pilot matrix is $\mathbf{a} = [\sqrt{2.3}, -\sqrt{2.3}]$, the light blue circle represents the pilot signal with $a_1 = \sqrt{2.3}$, and the brown circle represents the pilot signal with $a_2 = -a_1 = -\sqrt{2.3}$. The element value in \mathbf{a} changes according to the variation of fading channels, the transmitted symmetric pilot matrix \mathbf{x} is denoted as:

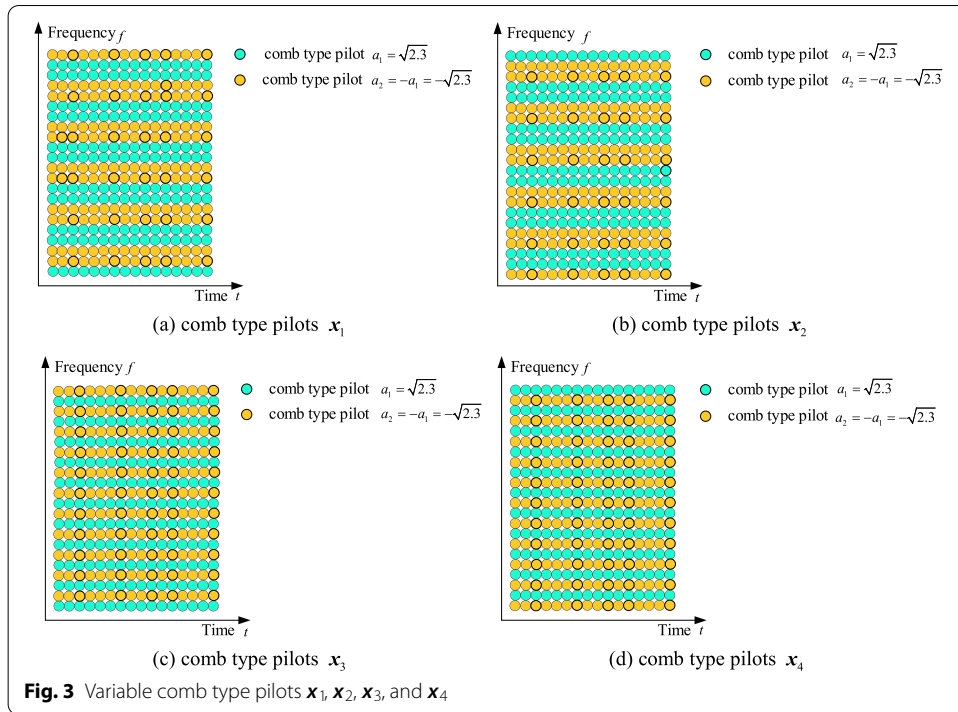


Fig. 3 Variable comb type pilots $\mathbf{x}_1, \mathbf{x}_2, \mathbf{x}_3,$ and \mathbf{x}_4

$$\mathbf{x} = \begin{bmatrix} \mathbf{x}_1 \\ \mathbf{x}_2 \\ \mathbf{x}_3 \\ \mathbf{x}_4 \end{bmatrix} = \begin{bmatrix} -a_1 & a_1 & a_1 & -a_1 \\ a_1 & -a_1 & -a_1 & a_1 \\ -a_1 & a_1 & -a_1 & a_1 \\ a_1 & -a_1 & a_1 & -a_1 \end{bmatrix}, \tag{9}$$

where the first kind of comb type pilot in \mathbf{x} is \mathbf{x}_1 , the second kind of comb type pilot is \mathbf{x}_2 , the third kind of comb type pilot is \mathbf{x}_3 , and the fourth kind of comb type pilot is \mathbf{x}_4 .

Supposing the transmitting OFDM symbols on each data subcarriers are $e_i (1 \leq i \leq N_d)$ and N_d denotes the number of transmitting OFDM symbols, which means $\mathbf{e}_i = [e_1, e_2, e_3, \dots, e_{N_d}]$. Under comb type \mathbf{x}_1 insertion, and pilot interval $n = 2$, the symmetric matrix of the transmitting OFDM symbols on four consecutive subcarriers λ_m are denoted as:

$$\lambda_m = \begin{bmatrix} A \\ s_{4m-3} \\ B \\ s_{4m-2} \\ B \\ s_{4m-1} \\ A \\ s_{4m} \end{bmatrix} = \begin{bmatrix} -a_1 & -a_1 & -a_1 & -a_1 \\ e_{16m-15} & e_{16m-14} & e_{16m-13} & e_{16m-12} \\ a_1 & a_1 & a_1 & a_1 \\ e_{16m-11} & e_{16m-10} & e_{16m-9} & e_{16m-8} \\ a_1 & a_1 & a_1 & a_1 \\ e_{16m-7} & e_{16m-6} & e_{16m-5} & e_{16m-4} \\ -a_1 & -a_1 & -a_1 & -a_1 \\ e_{16m-3} & e_{16m-2} & e_{16m-1} & e_{16m} \end{bmatrix}, \quad 1 \leq m \leq 124, \tag{10}$$

where m is the number of symmetric matrices in 2×2 MIMO-OFDM systems. The transmitting pilots on subcarriers are A and B . The transmitting OFDM symbols on four consecutive subcarriers are $s_{4m-3}, s_{4m-2}, s_{4m-1},$ and s_{4m} , respectively. When $m = 125$, the seventh and eighth line in matrix λ_m is all zero.

Table 1 The corresponding relation between f_d and t_c in AWGN channels

f_d (Hz)	t_c (s)
0.01	1.7905×10^3
0.05	71.6197
0.1	17.9049
0.2	4.4762
20	4.4762×10^{-4}
60	4.9736×10^{-5}
80	2.7976×10^{-5}

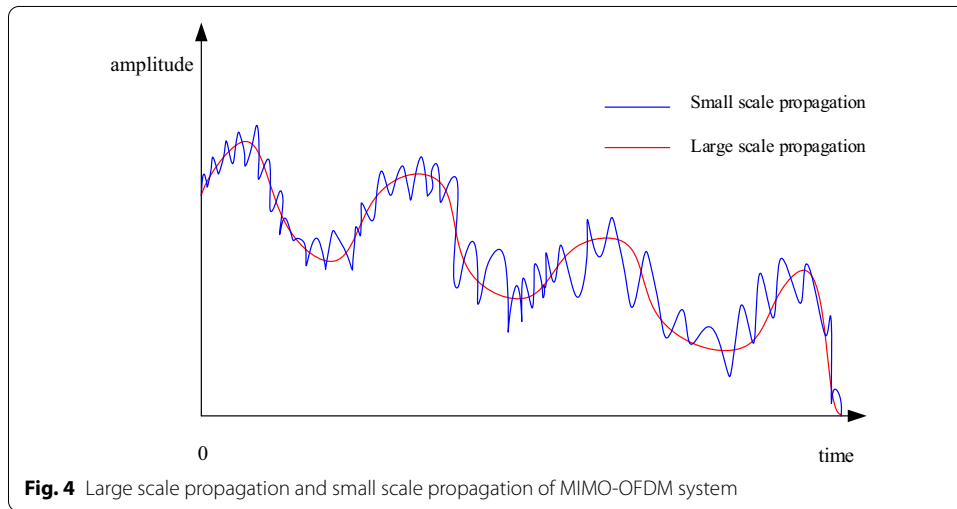


Fig. 4 Large scale propagation and small scale propagation of MIMO-OFDM system

3.2 Small scale propagation in MIMO-OFDM system

Under Rayleigh fading channel [21], the coherence time t_c of MIMO-OFDM system is defined as:

$$t_c = \frac{9}{16\pi f_d^2}, \tag{11}$$

where f_d is the Doppler frequency shift, and f_d is expressed as [22]:

$$f_d = \frac{v}{\lambda}, \tag{12}$$

where v is the speed of mobile station and λ is the wavelength. When the Doppler frequency shift f_d is 20 Hz, 60 Hz, 80 Hz, 120 Hz, 160 Hz, and 180 Hz, respectively, the corresponding coherence time t_c is 4.4762×10^{-4} s, 4.9736×10^{-5} s, 2.7976×10^{-5} s, 1.2434×10^{-5} s, 6.9941×10^{-6} s, and 5.5262×10^{-6} s, respectively. As f_d increases, t_c decreases gradually, and the multipath channel will experience deep fading. Table 1 shows the corresponding relation between f_d and t_c in AWGN channel. Figure 4 illustrates large scale propagation and small scale propagation of MIMO-OFDM systems. When f_d increases, it induces time selective propagation. The time selective propagation includes large-scale propagation and small-scale propagation. To suppress the ISI

Table 2 Parameters of MIMO-OFDM system

Parameters	Specifications
Modulation mode	BPSK/ QPSK/8PSK/16QAM/64QAM
System model	MIMO-OFDM
Transmitting antenna number	2
Receiving antenna number	2
CP length (subcarriers)	512
IFFT length (subcarriers)	2048
Pilot interval n	2, 4, 8, 20, 50, 100
Pilot insertion type	Comb type

which is caused by small-scale propagation, the pilots are inserted in comb type manner through the subcarriers in the frequency domain with variable pilots.

4 Simulation results and comparison analysis

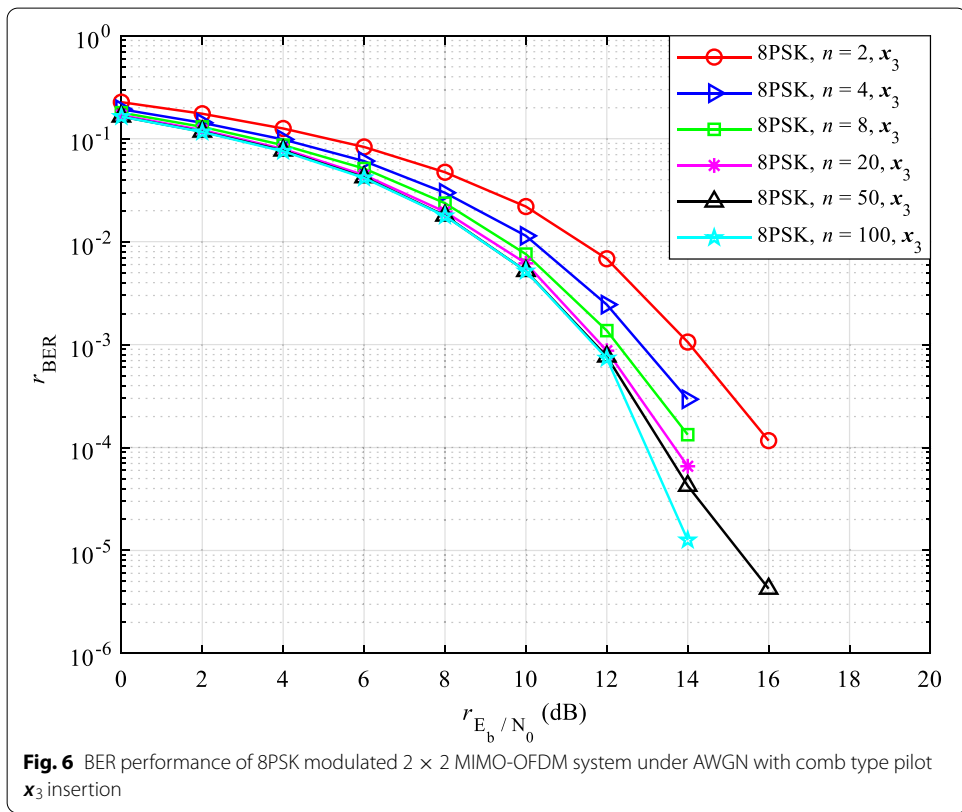
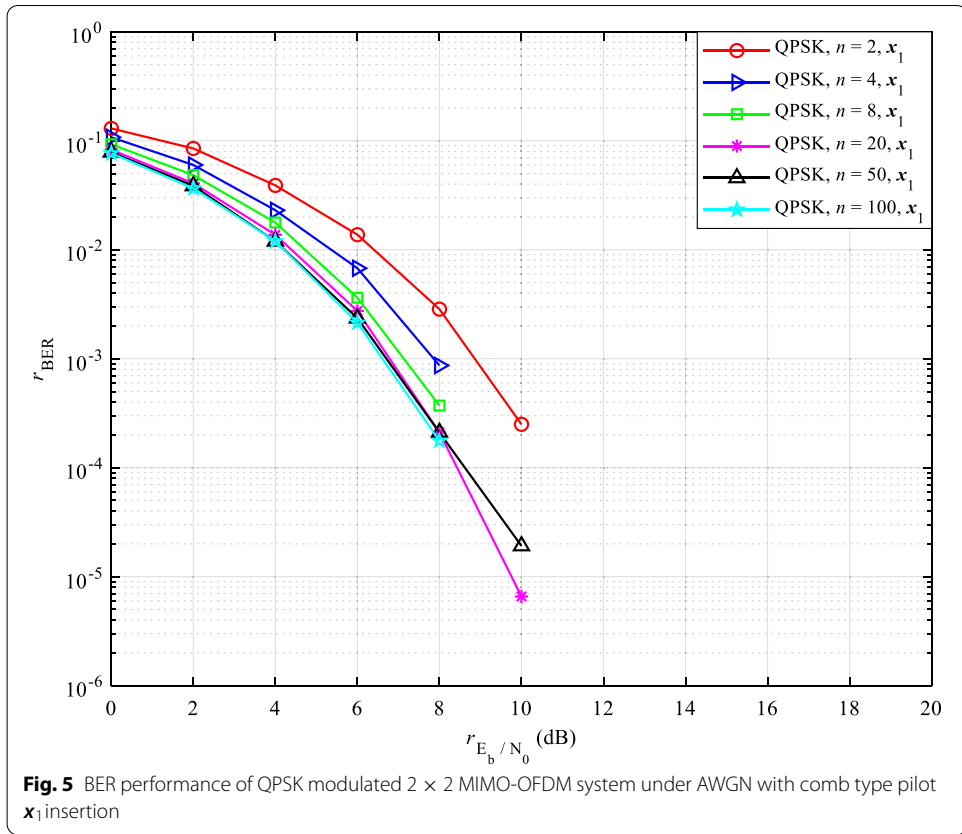
In MIMO-OFDM system, the transmitted signal and received signal are independent of each other, thus the probability of signal interference caused by AWGN or multipath is greatly reduced. The theoretical analysis would be verified through simulation. The simulation is performed in static AWGN channel and it adopts five kinds of modulation modes. The comb type pilots x_1 , x_2 , x_3 , and x_4 are inserted in the proposed MIMO-OFDM systems, and the parameters of MIMO-OFDM system are shown in Table 2.

The BER curve of the system could be drawn by making the statistics of BER for every OFDM frame under different SNR. In the statistical process of BER, the bit stream of each frame output by the constellation symbol demodulation module is compared with the bit stream contained in each frame transmitted, and the error bits are demodulated and accumulated to obtain the sum of the cumulative number of error bits per frame. And then the number of error bits in all transmitted OFDM data frames is accumulated, and the total number of bits transmitted in all transmitted OFDM data frames is calculated. The whole process that antenna transmit signals and antenna receive signals is cyclic, and the total number of error bits is obtained. With a certain fixed SNR, the calculated BER of the MIMO-OFDM system is denoted as:

$$r_{\text{BER}} = \frac{\sum_{u=1}^L N_u}{LN_t}, \quad (13)$$

where N_u is the number of error bits in the u th OFDM frame under the condition that the maximum number of cycles is L . Assuming that the MIMO-OFDM system transmitter transmits equal data bits in each OFDM transmitted in each frame is equal, and N_t represents the number of bits transmitted in each OFDM frame.

Figure 5. shows BER performance of QPSK modulated 2×2 MIMO-OFDM system under AWGN with comb type pilot x_1 insertion. As shown in Fig. 5, the $n = 2$ BER curve has the worst performance; $n = 4$ BER curve is the second; $n = 8$ BER curve is the third; $n = 20$, $n = 50$, and $n = 100$ BER curves nearly all have better BER performance. For example, at the target $r_{\text{BER}} = 10^{-3}$, $n = 50$ BER curve outperforms $n = 2$ BER curve 2.15 dB SNR gains.



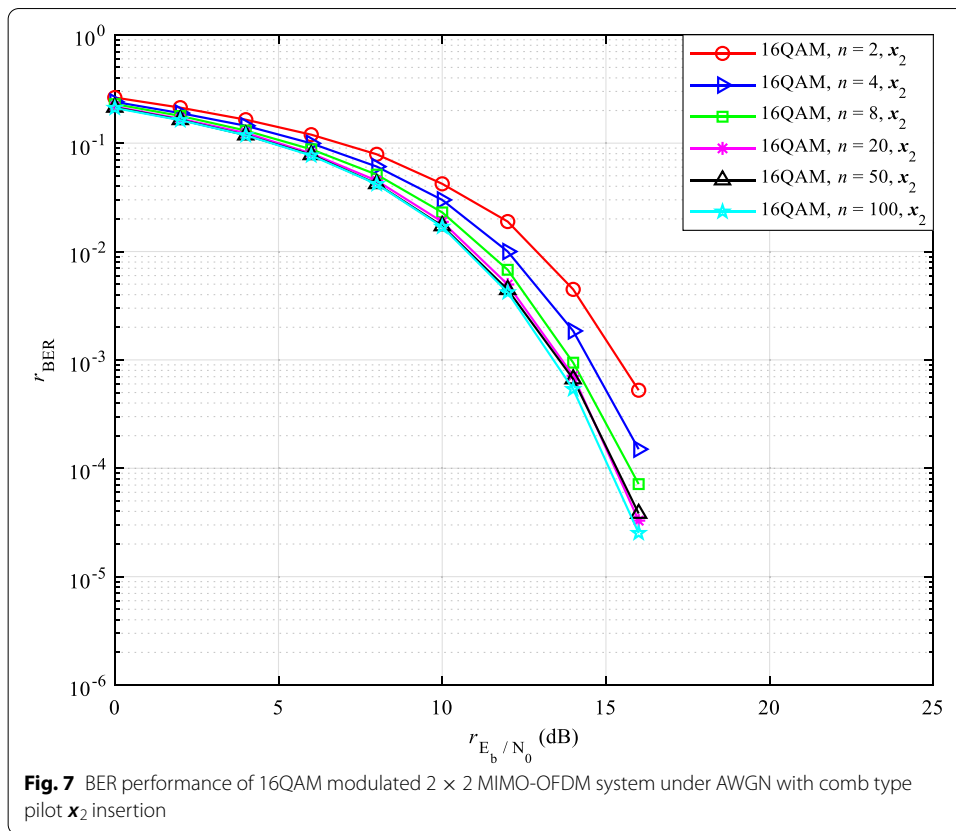
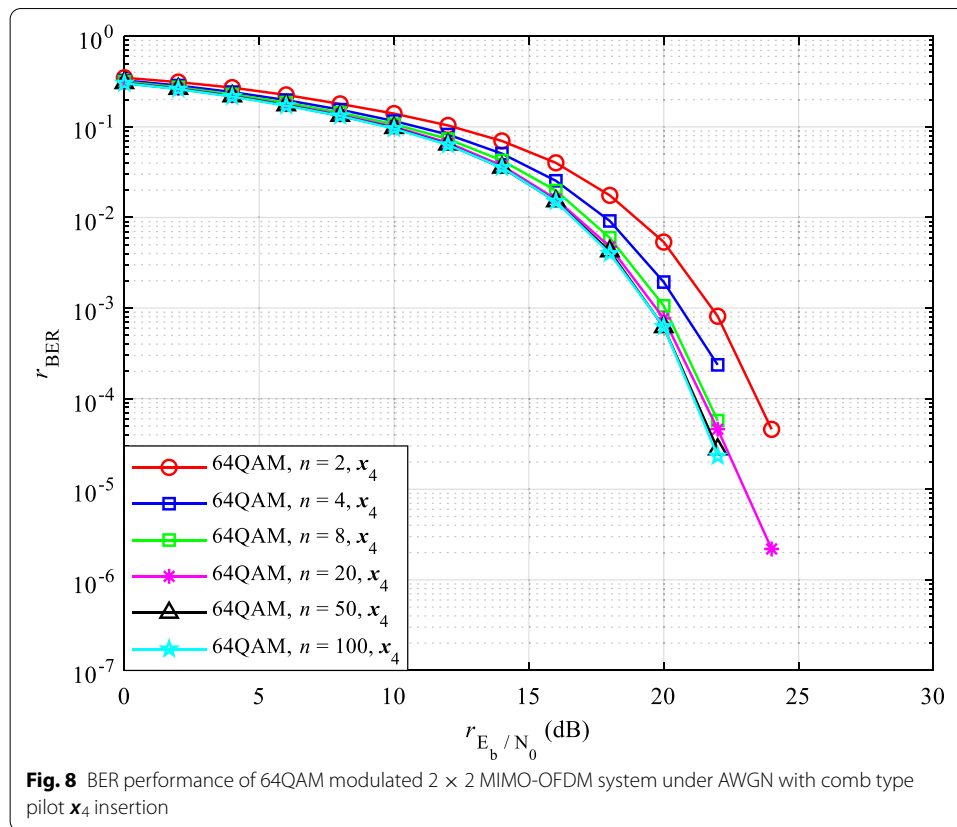


Figure 6. shows BER performance of 8PSK modulated 2×2 MIMO-OFDM system under AWGN with comb type pilot \mathbf{x}_3 insertion. As shown in Fig. 6, the $n = 2$ BER curve has the worst performance; $n = 4$ BER curve is the second; $n = 8$ BER curve is the third; $n = 20$ BER curve is the fourth; $n = 50$ BER curve is the fifth; and $n = 100$ BER curve has the best performance. At the target $r_{BER} = 10^{-3}$, the SNR gap between $n = 4$ BER curve and $n = 100$ BER curve is 1.1 dB.

Figure 7. shows BER performance of 16QAM modulated 2×2 MIMO-OFDM system under AWGN with comb type pilot \mathbf{x}_2 insertion. As shown in Fig. 7, $n = 2$ BER curve has the best performance; $n = 4$ BER curve is the second; $n = 8$ BER curve is the third. It can be seen that $n = 20$, $n = 50$, and $n = 100$ nearly all have better BER performance. At the target $r_{BER} = 10^{-3}$, $n = 8$ BER curve outperforms $n = 4$ BER curve about 0.8 dB SNR gains.

Figure 8. shows BER performance of 64QAM modulated 2×2 MIMO-OFDM system under AWGN with comb type pilot \mathbf{x}_4 insertion. As shown in Fig. 8, $n = 8$, $n = 20$, $n = 50$, and $n = 100$ near all have better BER performance. At the target $r_{BER} = 10^{-4}$, $n = 20$ BER curve outperforms $n = 2$ BER curve 2.4 dB SNR gains. In the paper, it is recommended that the optimal pilot interval value of P in the proposed variable pilot assisted MIMO-OFDM system is $P \in [8, 100]$.



5 Conclusion

This paper studies a variable pilot assisted channel estimation method in STBC MIMO-OFDM system with different modulation modes. The variable pilot patterns are proposed to estimate the transmitted OFDM symbols by effectively allocate comb type pilot sequences through the frequency subcarriers. The proposed variable pilot patterns work well for MIMO-OFDM systems. The novelty of the paper is that it saves the spectrum resources by using STBC and variable pilot insertion intervals. Moreover, the performance of MIMO-OFDM systems is improved as can be observed from the simulation results. In the future, we will apply the proposed variable pilot assisted channel estimation method in cognitive MIMO-OFDM systems [23, 24], ultra-wideband MIMO-OFDM systems [25], China multimedia mobile broadcasting MIMO-OFDM systems [26], massive MIMO-OFDM systems [27, 28], and underwater acoustic OFDM systems [29].

Abbreviations

AWGN: Additive white Gaussian noise; BER: Bit error rate; BPSK: Binary phase shift keying; CFR: Channel frequency response; CP: Cyclic prefix; CSI: Channel state information; FFT: Fast Fourier transform; ICI: Inter-carrier interference; IFFT: Inverse fast Fourier transform; ISI: Inter-symbol interference; LS: Least square; MIMO: Multiple input multiple output; MSE: Mean square error; OFDM: Orthogonal frequency division multiplexing; OTS: Optimal training sequences; P/S: Parallel to serial; QPSK: Quadrature phase shift keying; SNR: Signal-to-noise ratio; STBC: Space time block coding; STBD: Space time block decoding; S/P: Serial to parallel; 8PSK: 8-phase shift keying; 16QAM: 16-quadrature amplitude modulation; 64QAM: 64-quadrature amplitude modulation.

Acknowledgements

The authors thank Mingtong Zhang and Ruiguang Tang for their kind help and valuable suggestions in revising this paper.

Author contributions

QW, XZ, CW, and HC conceived the algorithm and designed the experiments; HC designed computer programs; QW and CW performed the experiments; HC prepared tables and figures; XZ and HC analyzed the experimental results; XZ and CW drafted the manuscript; QW, XZ, and HC revised the manuscript. All authors read and approved the final manuscript.

Authors' information

Qun Wu was born in Heze city, Shandong province, China, in 1998. She received the B.E. degree in electronic information engineering from Jiangxi University of Science and Technology, China, in 2020. She is currently pursuing the M.E. degree in information and communication engineering with Shandong University, China. Her current research interests include wireless communication theory and technology, intelligent information processing, and computer vision.

Xiao Zhou received the B.E. degree in automation from Nanjing University of Posts and Telecommunications, China, in 2003; the M.E. degree in information and communication engineering from Inha University, Korea, in 2005; and the Ph.D. degree in information and communication engineering from Tsinghua University, China, in 2013. She is currently an associate professor and a master's supervisor with Shandong University, Weihai, China. Her current research interests include wireless communication technology, image communication, digital image/video processing and analysis, intelligent information processing, computer vision, and artificial intelligence.

Chengyou Wang received the B.E. degree in electronic information science and technology from Yantai University, China, in 2004, and the M.E. and Ph.D. degrees in signal and information processing from Tianjin University, China, in 2007 and 2010, respectively. He is currently an associate professor and a master's supervisor with Shandong University, Weihai, China. His current research interests include digital image/video processing and analysis, intelligent information processing, computer vision, deep learning, artificial intelligence, and wireless communication technology.

Hai Cao received the B.S. degree in computer science and technology from Shandong University, Weihai, China, in 2003, and the M.E. degree in computer applications from Shandong University, China, in 2006. He is currently a lecturer with Shandong University, Weihai, China. His current research interests include software theory and engineering, digital image processing, machine learning, and wireless communications.

Funding

This work was supported in part by the Joint Fund of Shandong Provincial Natural Science Foundation (No. ZR2021LZHP003), in part by the Shandong Provincial Natural Science Foundation, China (Nos. ZR2020MF008, ZR2021MF060), in part by the 16th Student Research Training Program (SRTP) at Shandong University, Weihai (No. A21246), in part by the Education and Teaching Reform Research Project of Shandong University, Weihai (No. Y2021054), and in part by the Science and Technology Development Plan Project of Weihai Municipality in 2020.

Availability of data and materials

Not applicable.

Declarations

Competing interests

The authors declare that they have no competing interests.

Received: 2 October 2020 Accepted: 20 April 2022

Published online: 16 May 2022

References

1. F. Adachi, A. Bookajay, T. Saito, Y. Seki, Performance comparison of MIMO diversity schemes in a frequency-selective Rayleigh fading channel, in *Proceedings of the IEEE International Conference on Communication Systems*, Chengdu, China, pp. 62–66 (2018)
2. J. Zheng, R. Chen, Achieving transmit diversity in OFDM-IM by utilizing multiple signal constellations. *IEEE Access*. **5**, 8978–8988 (2017)
3. C.B. Papadias, G.J. Foschini, A space-time coding approach for systems employing four transmit antennas, in *Proceedings of the IEEE International Conference on Acoustics, Speech, and Signal Processing*, Salt Lake, UT, USA, vol. 4, pp. 2481–2484 (2001)
4. H. Huang, H. Viswanathan, G.J. Foschini, Multiple antennas in cellular CDMA systems: Transmission, detection, and spectral efficiency. *IEEE Trans. Wirel. Commun.* **1**(3), 383–392 (2002)
5. H. Alves, M. De Castro Tome, P. Nardelli, C. De Lima, M. Latva-Aho, Enhanced transmit antenna selection scheme for secure throughput maximization without CSI at the transmitter. *IEEE Access*. **4**, 4861–4873 (2016)
6. K. Sagar, P. Palanisamy, Optimal orthogonal pilots design for MIMO-OFDM channel estimation, in *Proceedings of the 5th IEEE International Conference Computing and Intelligence Systems*, Coimbatore, Tamil Nadu, India, pp. 1–4 (2014)
7. J.W. Kang, Y. Whang, H.Y. Lee, K.S. Kim, Optimal pilot sequences design for multi-cell MIMO-OFDM systems. *IEEE Trans. Wirel. Commun.* **10**(10), 3354–3367 (2011)
8. H. Al-Salih, M.R. Nakhai, T.A. Le, Enhanced sparse Bayesian learning-based channel estimation with optimal pilot design for massive MIMO-OFDM systems. *IET Commun.* **12**(17), 2174–2180 (2018)

9. S.J. Chern, Y.S. Huang, Y.G. Jan, R.H.H. Yang, Performance of the MIMO PRCP-OFDM system with orthogonal cyclic-shift sequences, in *Proceedings of the 20th IEEE International Symposium on Intelligent Signal Processing and Communication Systems*, Tamsui, New Taipei City, Taiwan, pp. 553–558 (2012)
10. J.A. Del Peral-Rosado, M.A. Barreto-Arboleda, F. Zanier, M. Crisci, G. Seco-Granados, J.A. Lopez-Salcedo, Pilot placement for power-efficient uplink positioning in 5G vehicular networks, in *Proceedings of the 18th IEEE International Workshop on Signal Processing Advances in Wireless Communications*, Sapporo, Japan, pp. 1–5 (2017)
11. T. Younas, J. Li, J. Arshad, On bandwidth efficiency analysis for LS-MIMO with hardware impairments. *IEEE Access*. **5**, 5994–6001 (2017)
12. Y. Seki, A. Boonkajay, F. Adachi, Adaptive MMSE-SVD to improve the tracking ability against fast fading, in *Proceedings of the 88th IEEE Vehicular Technology Conference*, Chicago, IL, USA, pp. 1–5 (2018)
13. Y. Seki, F. Adachi, Downlink capacity comparison of MMSE-SVD and BD-SVD for cooperative distributed antenna transmission using multi-user scheduling, in *Proceedings of the 86th IEEE Vehicular Technology Conference*, Toronto, ON, Canada, pp. 1–5 (2017)
14. L. Wang, Y. Kuang, J. Liu, Pilot-assistant subcarrier allocation in virtual MISO-OFDM system, in *Proceedings of the 12th IEEE International Conference on Information & Communication Technology and System*, Nanjing, China, pp. 713–716 (2010)
15. M.A. Youssefi, J. El Abbadi, Pilot-symbol patterns for MIMO OFDM systems under time varying channels, in *Proceedings of the 1st IEEE International Conference on Electro Information Technology*, Marrakech, Morocco, pp. 322–328 (2015)
16. W. Sun, W. Yang, L. Li, A simple channel estimation method in MIMO-OFDM systems with virtual subcarriers, in *Proceedings of the IEEE International Conference on Wireless Communications, Networking and Information Security*, Beijing, China, pp. 35–39 (2010)
17. L. Tang, Q. Tan, Y. Shi, C. Wang, Q. Chen, Adaptive virtual resource allocation in 5G network slicing using constrained Markov decision process. *IEEE Access*. **6**, 61184–61195 (2018)
18. A. Kenarsari-Anhari, L. Lampe, Power allocation for coded OFDM via linear programming. *IEEE Commun. Lett.* **13**(12), 887–889 (2009).
19. Z. Wang, S. Dang, D.T. Kennedy, Multi-hop index modulation-aided OFDM with decode-and-forward relaying. *IEEE Access*. **6**, 26457–26468 (2018)
20. C. Poongodi, P. Ramya, A. Shanmugam, BER analysis of MIMO OFDM system using M-QAM over Rayleigh fading channel, in *Proceedings of the International Conference on Communication and Computational Intelligence*, Erode, India, pp. 284–288 (2010)
21. G. Casu, F. Georgescu, M. Nicolaescu, A. Mocanu, A comparative performance analysis of MIMO-OFDM system over different fading channels, in *Proceedings of the 7th International Conference on Electronics, Computers and Artificial Intelligence*, Bucharest, Romania, pp. 1–4 (2015)
22. S.H. Aswini, B.N. Ardra Lekshmi, S. Sekhar, S.S. Pillai, MIMO-OFDM frequency offset estimation for Rayleigh fading channels, in *Proceedings of the 1st International Conference on Computational Systems and Communications*, Trivandrum, India, pp. 191–196 (2014)
23. C.N. Devanarayana, A.S. Alfa, Decentralized channel assignment and power allocation in a full-duplex cognitive radio network, in *Proceedings of the 13th IEEE Annual Consumer Communications and Networking Conference*, Las Vegas, NV, USA, pp. 829–832 (2016)
24. X. Zhou, W. Xu, X. Shi, J. Lin, Energy-efficient power loading with intercarrier and intersymbol interference considerations for cognitive OFDM systems, in *Proceedings of the 81st IEEE Vehicular Technology Conference*, Glasgow, United Kingdom, pp. 1–5 (2015)
25. N.M. Anas, S.K.S. Yusof, R. Mohamad, On the performance of SVD estimation in Saleh-Valenzuela channel for UWB systems, in *Proceedings of the IEEE Region 10 Annual International Conference*, Xi'an, China, pp. 1–5 (2013)
26. F. Hu, Y. Wang, L. Jin, Robust MIMO-OFDM design for CMMB systems based on LMMSE channel estimation, in *Proceedings of the 5th IEEE International Conference on Electronics Information and Emergency Communication*, Beijing, China, pp. 59–62 (2015)
27. K. Zhang, W. Tan, G. Xu, C. Yin, W. Liu, C. Li, Joint RRH activation and robust coordinated beamforming for massive MIMO heterogeneous cloud radio access networks. *IEEE Access*. **6**, 40506–40518 (2018)
28. C. Xu, Y. Hu, C. Liang, J. Ma, L. Ping, Massive MIMO, non-orthogonal multiple access and interleave division multiple access. *IEEE Access*. **5**, 14728–14748 (2017)
29. R. Jiang, X. Wang, S. Cao, J. Zhao, X. Li, Deep neural networks for channel estimation in underwater acoustic OFDM systems. *IEEE Access*. **7**, 23579–23594 (2019)

Publisher's Note

Springer Nature remains neutral with regard to jurisdictional claims in published maps and institutional affiliations.